# Surface Studies of the Rearrangement of End Groups of a Polymer by ToF−SIMS and AFM

**Lin Li, Kai-Mo Ng, Chi-Ming Chan,* Ji-Yun Feng, and Xin-Miao Zeng**

*Department of Chemical Engineering, Advanced Engineering Materials Facility, Hong Kong University of Science and Technology, Clear Water Bay, Hong Kong*

**Lu-Tao Weng**

*Materials Characterization and Preparation Facility, Hong Kong University of Science and Technology, Clear Water Bay, Hong Kong*

*Received July 15, 1999; Revised Manuscript Received April 11, 2000*

ABSTRACT: The polymer (BA-C8) was prepared by condensation polymerization of bisphenol A and 1,8-dibromooctane. The bromine atoms that were attached to the ends of the polymer chains could be used to determine the distribution of the end groups on the surface of BA-C8 polymer films. The surface morphology was studied using atomic force microscopy (AFM) tapping mode phase imaging. Direct observation of the growth process of a spherulite indicates that the diameter of the spherulite increases with time. The spatial distribution of the end group, Br, was determined by time-of-flight secondary ion mass spectrometry (ToF−SIMS) chemical imaging. For the amorphous films, a homogeneous distribution of the end groups at the surface was found, while for the semicrystalline films the end groups rearranged and preferentially segregated at the surface of the boundaries and the eyes of the spherulites.

## Introduction

Time-of-flight secondary ion mass spectrometry (ToF−SIMS) is now widely used to characterize the surface chemical structure of different materials[1,2] because the secondary molecular ions that are emitted from the surface are very characteristic of the functional groups and the chemical structures present at the uppermost surface.[3−6] It has been applied to the investigation of the surface molecular weights and end groups,[6−11] surface crystallization,[12] specific interactions,[13] and quantitative analysis[14−16] of polymers. Recently, with the use of a liquid metal ion gun, ToF−SIMS chemical imaging[12,17,18] of polymer surfaces with submicron lateral resolution has been achieved. This chemical imaging capability is especially useful for studying the surface chemical distributions, such as the distribution of end groups.

Many polymers are semicrystalline with polymer chains folding to form the lamellae of spherulites. It is commonly accepted that chain end groups cannot fold into the lamellae of spherulites during crystallization because the chemical structures of the chain end and main chain are different. Therefore, the chain end groups of a polymer play an important role in controlling the morphology and properties of the surface. The preferential segregation of the chain end groups to an amorphous polymer surface may be explained by the larger free volume fraction at the surface compared with that of the bulk and the higher thermal polymer chain mobility at the surface.[19−21] However, the influence of end groups on the surface morphology and the end group distribution during crystallization have not been studied.

Atomic force microscopy (AFM) has been proven to be useful in studying the dynamic crystallization processes of polymers due to the development of tapping mode and phase imaging.[22,23] AFM can produce high-resolution images of surface topography and nanostructures. For example, the growth rates of a spherulite and the individual lamella at the growth fronts of a poly(hydroxybutyrate-*co*-valerate) copolymer have been determined by AFM.[22] More recently, a direct observation of the dynamic processes of the primary and secondary nucleations of the BA-C8 polymer films has clearly indicated the thermal motion and migration of the chain segments during crystallization. [23]

In this study, the distribution and reorientation of the chain end groups, Br, at the surface of BA-C8 polymer thin films were studied using AFM and ToF−SIMS.

## Experimental Section

**Polymer Materials.** The BA polymer was synthesized by condensation polymerization as previously reported.[24] A very small excess amount of 1,8-dibromooctane was used in order to keep the Br atom as the end group. The structure, the glass transition temperatures, the weight-average molecular weights, and the polydispersity indexes of the polymer that were measured from gel permeation chromatography have also been reported.[24] Thin films were prepared by spin coating a 30 mg $mL^{-1}$ polymer−chloroform solution at 3000 rpm onto silicon wafer surfaces (∼10 mm × 10 mm). The samples were dried in a vacuum at 25 ± 1 °C for 15 min. The thickness of the amorphous BA-C8 films was estimated to be about 300 nm by a profilometer.

**AFM.** AFM phase images were obtained by using a NanoScope III MultiMode AFM of Digital Instruments at room temperature. Both height and phase images were recorded simultaneously using the retrace signal. Si tips with a resonance frequency of approximately 300 kHz and a spring constant of 40 mN $cm^{-1}$ were used, and the scan rate was in the range 0.5−1.2 Hz.

**ToF−SIMS.** The ToF−SIMS measurements were performed on a Physical Electronics PHI 7200 ToF−SIMS spectrometer. The chemical images of the BA-C8 polymer films were acquired in the negative mode using a $^{69}Ga^{+}$ liquid metal ion source operating at 25 keV. The mapped area was 100 $\mu$m × 100 $\mu$m with a maximum of 50 frame scans.[17] The total ion

* To whom correspondence should be addressed.

10.1021/ma991142k CCC: $19.00 
Published on Web 06/30/2000

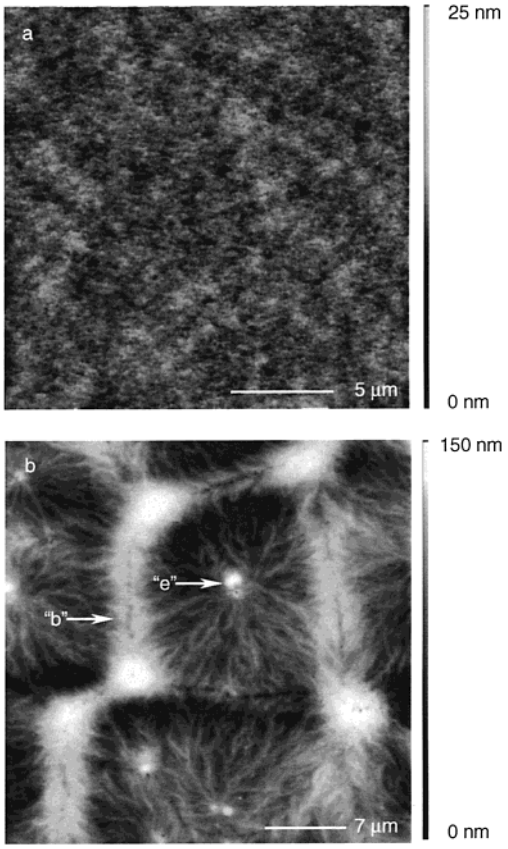


**Figure 1.** Surface topography of the BA-C8 thin films: (a) in the amorphous state and (b) in the semicrystalline state.

dose was lower than $4 \times 10^{12}$ ions/cm$^2$. The vacuum was about $1.5 \times 10^{-9}$ Torr. The semicrystalline BA-C8 polymer thin films were prepared by annealing the amorphous BA polymer films at 25 °C for different times. Amorphous BA-C8 polymer thin films were used after spin casting and dried in a vacuum for about 15 min.

## Results and Discussion

**Surface Morphology Changes.** The BA-C8 polymer thin films freshly prepared by spin-casting the polymer solution onto Si wafers are amorphous. When the amorphous films are allowed to crystallize at a temperature above the polymer's glass transition temperature, the polymer chains relax and change their conformation, folding into the lattice of lamellae and forming spherulites. The difference between the surface morphology of the amorphous and semicrystalline BA-C8 films is significant and can be observed using AFM. Parts a and b of Figure 1 show the surface morphology of the BA-C8 polymer films in the amorphous and semicrystalline states, respectively. In the amorphous state the surface of the BA-C8 polymer thin film is very smooth, with a surface roughness below 25 nm in an area of 20 $\mu$m × 20 $\mu$m. After the BA-C8 polymer had crystallized at 25 °C for 1 week, the surface of the thin film became rough. Spherulites with two characteristic eyes, "e" and the boundaries among the spherulites, "b" can be clearly seen, as shown in Figure 1b. Lamellar sheaves of the spherulites can also be observed.

In situ observations on the dynamic morphology changes of the BA-C8 films can provide detailed information on the polymer crystallization process. Figure 2 shows a series of AFM phase images taken during the growth of a stack of lamellae forming a spherulite of

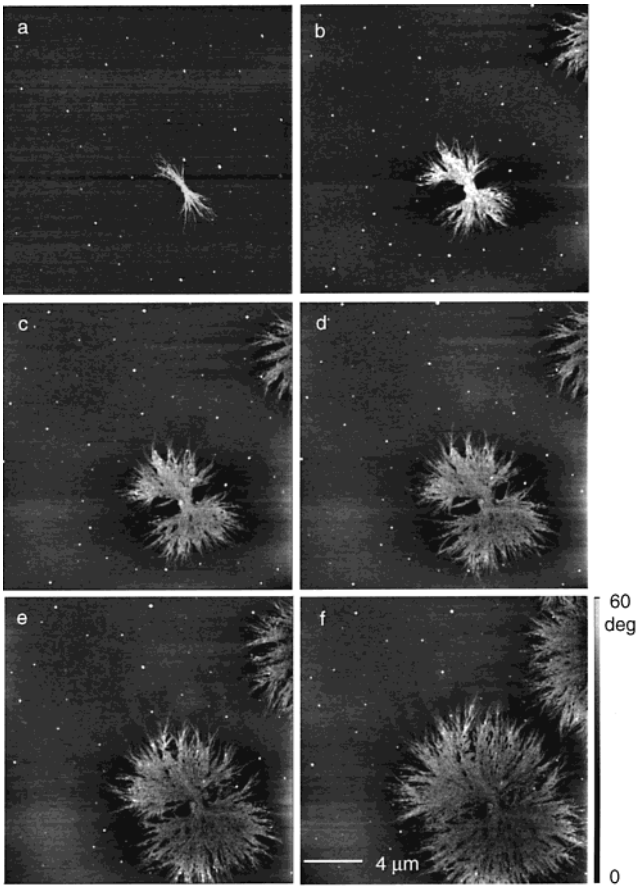


**Figure 2.** A series of AFM phase images of a spherulite growing on the surface of a BA-C8 polymer thin film.

the BA-C8 polymer. Figure 2a shows a stack of lamellae at the early stage of the growth. As the dominant initial lamellae grow, they induce secondary nuclei and splay apart from each other. As the growth continues the initial lamellae gradually develop into a lamellae sheaf and then a spherulite skeleton, as shown in parts a−e of Figure 2. After about 10 h, a spherulite is developed, as shown in Figure 2f. The envelope of the developing spherulite is not smooth, unlike those of other semicrystalline polymers observed using optical microscopy. The growth front of the developing spherulite looks like a hedgehog.

**Surface Chemical Structures.** The structure and the characteristic negative ions of the BA-C8 polymer are shown in Scheme 1.

**Scheme 1. Some Characteristic Negative Ions of the BA-C8 Polymer**

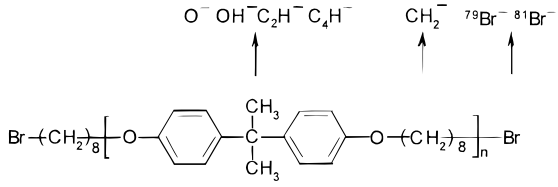


In the negative ToF−SIMS spectra of the BA-C8 polymer, the characteristic fragments of the end groups are $-^{79}Br^-$ at $m/z = 79$ amu and $-^{81}Br^-$ at $m/z = 81$ amu. The characteristic fragments of the rigid segment are $-O^-$ at $m/z = 16$ amu, $-OH^-$ at $m/z = 17$ amu, $-C_2H^-$ at $m/z = 25$ amu, and $-C_4H^-$ at $m/z = 49$ amu, and the characteristic fragment for the flexible segment

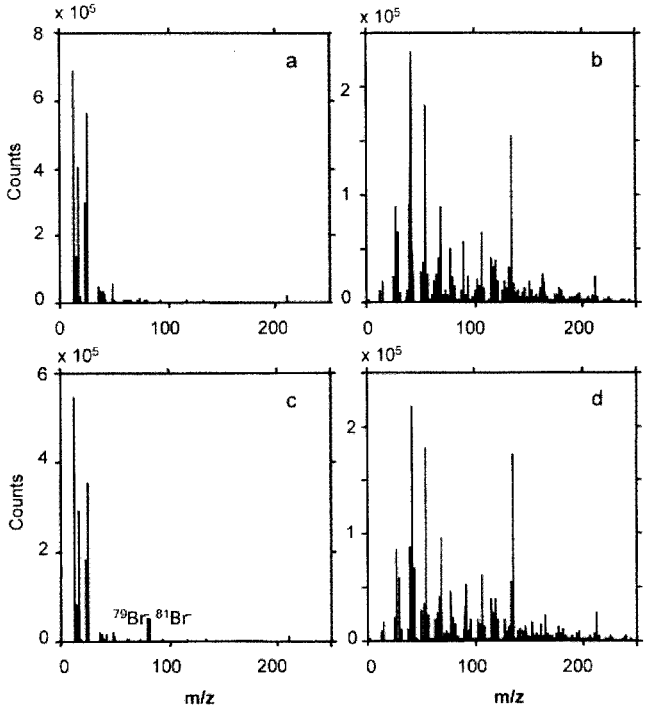


**Figure 3.** ToF−SIMS spectra of the BA-C8 polymer: (a) negative spectrum of a BA-C8 amorphous film; (b) positive spectrum of a BA-C8 amorphous film; (c) negative spectrum of a BA-C8 semicrystalline film; (d) positive spectrum of a BA-C8 semicrystalline film.

is $-CH_2^-$ at $m/z = 14$ amu, as shown in Scheme 1 and Figure 3. There are no distinguishable differences in the high-mass-resolution spectra between the amorphous and semicrystalline polymer films except for the intensities of the end groups: $-^{79}Br^-$ and $-^{81}Br^-$. To semiquantitatively analyze the difference in chemical composition between the semicrystalline and amorphous films of the BA-C8 polymer, the normalized intensity ratios, $I_n$, of the semicrystalline and amorphous BA-C8 samples are compared. $I_n$ is defined as

$$I_n = \left(\frac{I_i^c}{I_t^c}\right) \Big/ \left(\frac{I_i^a}{I_i^a}\right) \quad (1)$$

where, $I_i^c$ and $I_t^c$ are, respectively, the intensity of the peak at $m/z = i$ amu and the total intensity of the mass range $m/z = 2-500$ amu for the semicrystalline BA-C8 films. $I_i^a$ and $I_t^a$ are the same as $I_i^c$ and $I_t^c$ but for the amorphous BA-C8 films. The values of $I_n$ are very close to 1 for the positive secondary ions, as shown in Figure 4a. For the negative ions, the values of $I_n$ at $m/z = 79$ and 80 amu ($-^{79}Br^-$ and $-^{81}Br^-$) increase by a factor greater than 15. However, the values of $I_n$ for the other negative ions show almost no change, as shown in Figure 4b. These results show the end groups can segregate to the surface during crystallization.

**The Distribution of End Groups.** The distribution of the end groups at the surface can be determined even though the concentration of bromine is very low and cannot be detected by X-ray photoelectron spectroscopy (XPS) (cf., Figure 5) because the Br negative ion can be detected in very low concentrations in ToF−SIMS analysis.[25] The surface topography of the amorphous and semicrystalline BA-C8 thin films are determined using AFM, as shown in Figure 6, parts a−c. The chemical images of the BA-C8 films obtained by mapping the characteristic fragments of the end groups, the $-^{79}Br^-$ and $-^{81}Br^-$ peaks at $m/z = 79$ and 81 amu, are shown in Figure 6, parts d−f. Initially, the polymer chains in a freshly prepared BA-C8 film exist as random coils. The sample surface is very smooth, as shown in Figure 6a and the ToF−SIMS chemical image shows a homogeneous distribution of Br, as shown in Figure 6d. After about 10 h at 25 °C, a spherulite of ~10 $\mu$m in diameter is observed in the AFM image (cf., Figure 2f and Figure 6b). The relative height change of the BA-C8 film, which is due to the material constriction as a result of crystallization, is about 100 nm. A comparison between the AFM topographic image (cf., Figure 6b) and the ToF−SIMS chemical image (cf., Figure 6e) reveals the size of the spherulite to be similar to the sizes of the ToF−SIMS images showing higher Br concentrations. The surface of a BA-C8 polymer film which has been isothermally crystallized at room temperature for

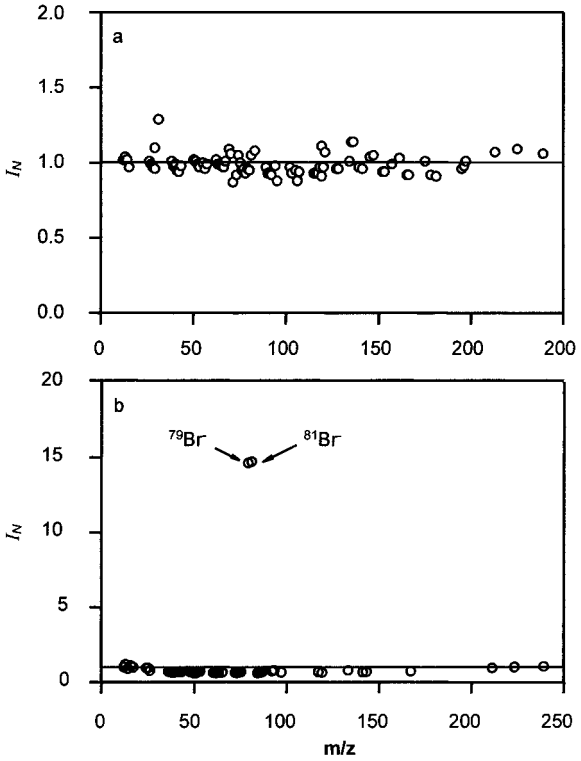


**Figure 4.** Comparison of surface compositions between the crystalline and amorphous BA-C8 polymer films: (a) ratios of the positive ToF−SIMS peaks; (b) ratios of the negative ToF−SIMS peaks.

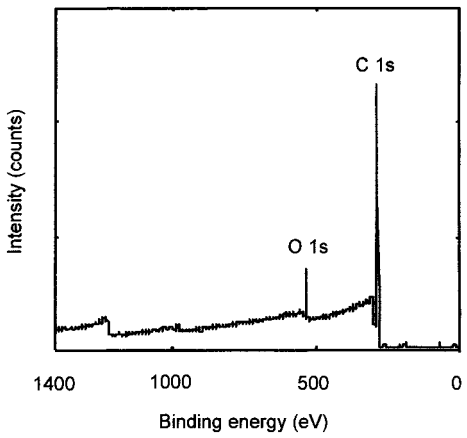


**Figure 5.** XPS survey spectra of the BA-C8 thin film.

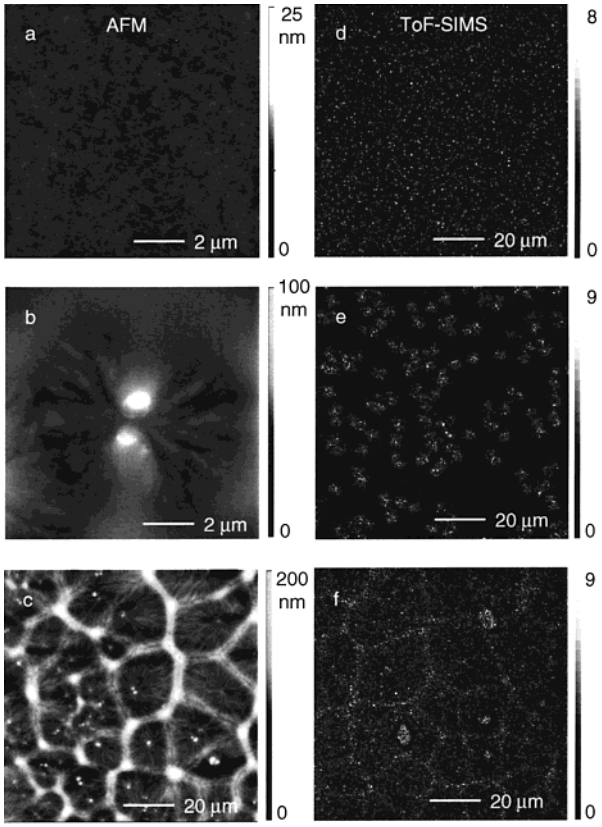


**Figure 6.** Surface morphology and end group distributions of the BA-C8 polymer films: (a and d) freshly prepared films; (b and e) films after isothermal crystallization at 25 °C for approximately 10 h; (c and f) films after isothermal crystallization at 25 °C for approximately 1 week.

1 week, shows a relative height change of the surface of ~200 nm, as shown in Figure 6c. The areas at the edges of the spherulites and the eyes at the centers of the spherulites are higher than other areas. The ToF−SIMS chemical image, as shown in Figure 6f, indicates the aggregation of the bromine end groups at the boundaries and the eyes of the spherulites.

The aggregation and rearrangement of the bromine end groups at the surface of the semicrystalline BA-C8 polymer film can be caused by thermodynamic as well as kinetic factors. Crystallization induces the migration and rearrangement of the chain segments and end groups on the surface of the BA-C8 polymer film. It is known that the free energy of a crystalline surface, $\gamma_c$, and the free energy of an amorphous surface, $\gamma_a$, are related by the following equation[26]

$$\gamma_c = (\rho_c/\rho_a)^{\beta}\gamma_a \qquad (2)$$

where $\rho_c$ and $\rho_a$ are the densities of the crystalline and the amorphous components, respectively. Usually, $\beta = 3.0-4.5$ and $\rho_c > \rho_a$, hence the free energy of a crystalline surface can be much higher than that of an amorphous surface. Crystallization increases the free energy of the surface and hence will promote the migration of the end groups to the surface.

Images of the detailed lamellar structures obtained using AFM tapping mode phase imaging are shown in Figure 7. Figure 7a shows the topographic image of a mature spherulite with two characteristic eyes (“e”), boundaries (“b”) and lamellar stacks (“s”). Figure 7b is the AFM phase image of the detailed structure of the

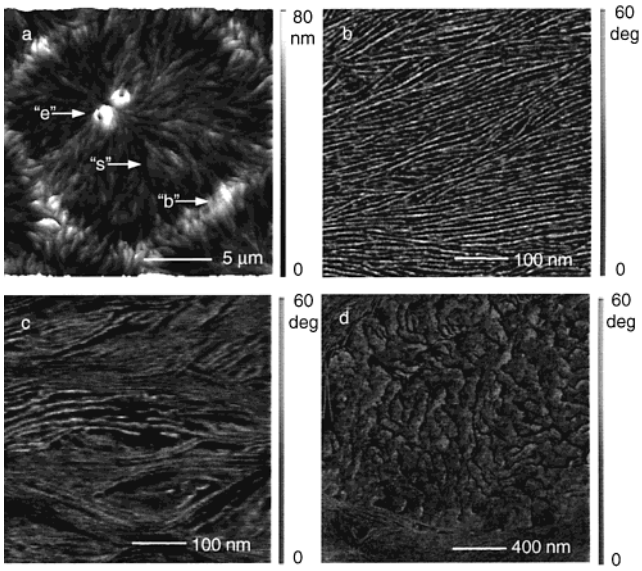


**Figure 7.** Detailed structures of the BA-C8 polymer films: (a) a mature spherulite; (b) lamellar stacks; (c) boundaries among spherulites; (d) the eye at the center of a spherulite.

lamellar stacks. It can be seen that the amorphous areas among the "edge-on” lamellae of the lamellar sheaf are relatively small. These dark areas consist of amorphous materials. However, there are more defects among the boundaries of the spherulites as shown in Figure 7c. The detailed lamellar structures of the eye of a spherulite, as shown in Figure 7d, indicate that the lamellae within the eyes are “flat-on” lamellae surrounded by “edge-on” lamellae.

The distribution and rearrangement of the bromine end groups at the boundaries and eyes of spherulites may be driven by the exclusion of the end groups from the lamellar structure. Consequently, the end groups are expelled and oriented at the amorphous areas among the lamellae of a spherulite, as illustrated in Scheme 2. It is also reasonable to conclude that the

**Scheme 2. Illustration of Bromine End-Group Distributions**

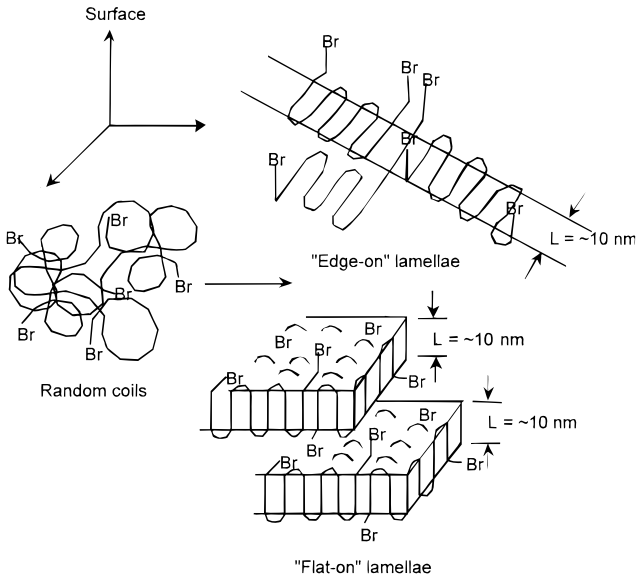


bromine end groups migrate to the defect areas at the boundaries among spherulites and congregate on the surfaces of the flat-on lamellae of the eyes of spherulites.

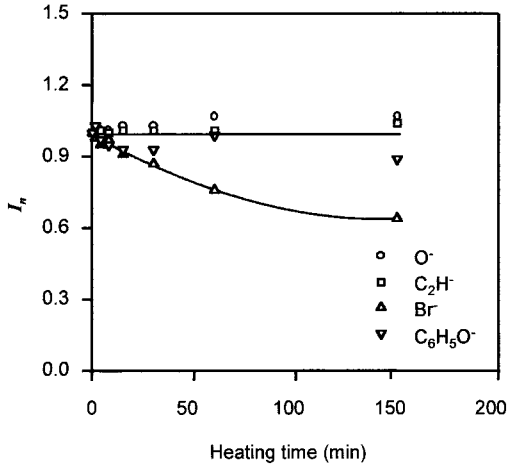


**Figure 8.** Normalized intensities of the characteristic negative ions as a function of heating time.

The AFM and ToF−SIMS results suggest that the segments and end groups of the BA-C8 polymer can rearrange their conformation at temperatures above the polymer's glass transition temperature. They also suggest that the surface morphology and chemical structure are governed by the dynamic process of polymer chain arrangement. This dynamic process can be very slow for some polymer materials, as is the case for the BA-C8 polymer.

**End Group Rearrangement.** The surface temperature increase was estimated to be about 7 °C by a thermocouple when a 150-W lamp heated the sample surface for 30 min at an ambient environment. A sequence of ToF−SIMS measurements was performed on the same area of the same sample at different times with the lamp aiming at the surface of the sample in the analysis chamber. The normalized intensity, $I_n$, of the characteristic negative fragment $i$ measured at time, $t$, can be expressed as

$$I_n = \frac{I_i(t)/I_t(t)}{I_i(t=0)/I_t(t=0)} \qquad (3)$$

where $I_i(t)$ and $I_t(t)$ are the absolute intensity of the characteristic negative fragment $i$ and the total intensity, respectively both measured at time $t$. $I_i(t = 0)$ and $I_t(t = 0)$ are the absolute intensity of the characteristic negative fragment ($i$) and the total intensity measured, respectively, at time $t = 0$. The ToF−SIMS spectra of the BA-C8 polymer films at different measurement times are similar to each other, except in the intensities of the end group ions, $-^{79}Br^-$ and $-^{81}Br^-$. The influence of the surface temperature on the migration of the bromine end groups at the surface of a BA-C8 polymer film is presented in Figure 8. A remarkable decrease in the normalized intensity of the end group ions is observed as the heating time increases. This is consistent with the fact that a higher temperature increases the mobility of the polymer chains. As the temperature of the surface increases, the crystalline structure, as shown in Scheme 2, can be disturbed. The randomization of the top layer of the film can cause a significant decrease in the Br concentration.

## Conclusion

In this work, the influence of bromine end groups on the surface morphology of the amorphous and semicrystalline films of BA-C8 polymer was evaluated. The end groups are shown to be homogeneously distributed on the surface of an amorphous BA-C8 film. The surface chemical imaging of a semicrystalline BA-C8 polymer film reveals that the end groups are preferentially segregated on the surfaces of the eyes and boundaries of the spherulites because the bromine end groups are expelled to the surface of the lamellae during crystallization. The dynamic rearrangement of the bromine end groups on the surfaces of the BA-C8 polymer films has been studied using ToF−SIMS. The normalized intensities of the bromine end group ions are particularly sensitive to changes in surface temperature.

**Acknowledgment.** This work was supported by the Hong Kong Government Research Grant Council under Grant No. HKUST 9123/97P.

## References and Notes

(1) Briggs, D. *Surface Analysis of Polymers by XPS and Static SIMS*; Cambridge University Press: New York, 1998.
(2) Chan, C. M. *Polymer Surface Modification and Characterization*; Hanser: New York, 1994.
(3) Chen, X.; Gardella, J. A., Jr.; Ho, T.; Wynne, K. J. *Macromolecules* **1995,** *28,* 1635.
(4) Chen, X.; Gardella, J. A. Jr.; Cohen, R. E. *Macromolecules* **1994,** *27,* 2206.
(5) Hearn, M. J.; Ratner, B. D.; Briggs, D. *Macromolecules* **1988,** *21,* 2950.
(6) Galuska, A. A. *Surf. Interface Anal.* **1997,** *25,* 1.
(7) Davies, M. C.; Lynn, R. A. P.; Davis, S. S.; Hearn, J.; Wattes, J. F.; Vickerman, J. C.; Johnson, D. *J. Colloid Interface Sci.* **1993,** *156,* 229.
(8) Vanden Eynde, X.; Bertrand, P.; Dubois, P.; Jerome, R. *Macromolecules* **1998,** *31,* 6409.
(9) Vanden Eynde, X.; Bertrand, P.; Jerome, R. *Macromolecules* **1997,** *30,* 6407.
(10) Vanden Eynde, X.; Bertrand, P. *Surf. Interface Anal.* **1998,** *26,* 579.
(11) Leeson, A. M.; Alexander, M. R.; Short, R. D.; Briggs, D.; Hearn, M. J. *Surf. Interface Anal.* **1997,** *25,* 261.
(12) Reichlmaier, S.; Bryan, S. R.; Briggs, D. *J. Vac. Sci. Technol.* A **1995,** *13,* 1217.
(13) Li, L.; Chan, C. M.; Weng, L. T.; Xiang, M. L.; Jiang, M. *Macromolecules* **1998,** *31,* 7248.
(14) Briggs, D.; Davies, M. C. *Surf. Interface Anal.* **1997,** *25,* 725.
(15) Galuska, A. A. *Surf. Interface Anal.* **1996,** *24,* 380.
(16) Briggs, D.; Ratner, R. D. *Polym. Commun.* **1988,** *29,* 6.
(17) Weng, L. T.; Smith, T. L.; Feng, J. Y.; Chan, C. M. *Macromolecules* **1998,** *31,* 928.
(18) Lhoest, J. B.; Bertrand, P.; Weng, L. T.; Dewez, J. L. *Macromolecules* **1995,** *28,* 4631.
(19) Teraya, T.; Takahara, A.; Kajiyama, T. *Polymer* **1990,** *31,* 1149.
(20) Mayes, A. M. *Macromolecules* **1994,** *27,* 3114.
(21) Kajiyama, T.; Tanaka, K.; Takahara, A. *Macromolecules* **1995,** *28,* 3482.
(22) Hobbs, J. K.; McMaster, T. J.; Miles, M. J.; Barham. P. J. *Polymer* **1998,** *39,* 2437.
(23) Li, L.; Chan, C. M.; Li, J. X.; Ng, K. M.; Yeung, K. L.; Weng, L. T. *Macromolecules* **1999**, *32,* 8024.
(24) Li, L.; Chan, C. M.; Ng, K. M.; Weng, L. T. submitted to *Macromolecules*.
(25) Vanden Eynde, X.; Matyjaszewski, K.; Bertrand, P. *Surf. Interface Anal.* **1998,** *26,* 569.
(26) Brandrup, J.; Immergut, E. H. *Polymer Handbook*; Wiley: New York 1989.

MA991142K